# Fatigue and Fracture Behavior of an Aluminum-Lithium Alloy 8090-T6 at Ambient and Cryogenic Temperature

Y.B. XU, L. WANG, Y. ZHANG, Z.G. WANG, and Q.Z. HU

An investigation has been made of the fatigue and fracture behavior of an Al-Li-Cu-Mg-Zr 8090-T6 alloy at room (300 K) and liquid nitrogen (77 K) temperatures. The fatigue and fracture strengths, as well as ductility of the alloy, have been found to increase with decreasing temperature. The observations by scanning electron microscopy (SEM) and transmission electron microscopy (TEM) reveal that the changes in fatigue and fracture behavior with temperature are considered to be associated with the change in the deformation and fracture modes. It has been found that the occurrence of the localized shear deformation bands in which the hard precipitates are sheared by moving dislocations is responsible for the reduction of fatigue and fracture strengths as well as ductility of the alloy at room temperature. However, the improvement of both strength and ductility of the alloy at liquid nitrogen temperature might be attributed to the deeper and larger delamination that occurred on the fracture surface.

## I. INTRODUCTION

OVER the past few years, much attention has been paid to the development and application of aluminum-lithium alloys because of their high elastic modulus, low density, good resistance to propagation of fatigue cracks, as well as high strength. Unfortunately, the addition of lithium into the alloy can lead to decrease of both toughness and ductility that restricts further development and application. Recent investigations indicate that aluminum-lithium alloys display enhanced toughness and an improved strength-toughness relationship at low temperature.[1-6] It would be expected that aluminum-lithium alloys are attractive candidate materials for application in advanced aerospace structures at low temperature, such as liquid-hydrogen, liquid-oxygen, and natural gas fuel tanks, especially for existing and future transatmospheric and hypersonic aircraft applications. Therefore, the investigation on the fatigue behavior of alloy at low temperature is considered to be very significant and necessary but has not been reported so far. The purpose of the present study is to examine fatigue and fracture behavior of an aluminum-lithium alloy 8090-T6 at ambient and liquid nitrogen temperatures.

## II. MATERIALS AND PROCEDURES

An alloy, of composition similar to 8090, (in weight percent) 2.56 pct Li, 1.44 pct Cu, 1.18 pct Mg, 0.15 pct Zr, 0.009 pct Fe, 0.05 pct Si, balance Al, was selected for the present study.

An ingot of this alloy was prepared in 10 Kg heats by inductive smelting under high-purity argon at about 0.7 atm pressure and casting into a graphite mold. The ingots were scalped off the surface layer and homogenized at 400 °C for 16 hours and then 515 °C for 10 hours. After preheating at 450 °C for 2 hours, the ingots were extruded into bars 18 mm in diameter which were then hot rolled into 4.5-mm-thick plates. Both fatigue and tensile specimens were taken from the plate in *L-T* orientation.

Specimens of the alloy were solutionized at 525 °C for 1 hour. Following the solution heat treatment, the alloy was quenched in iced water and then aged at 190 °C for 16 hours to develop a peak precipitation hardening (T6).

An hour-glass type of fatigue specimen (Figure 1) was machined. In order to observe the deformation characteristics on the surface, the specimens were carefully polished with diamond paste before testing.

Fatigue tests under load control were conducted on a Schenck Servohydraulic machine at room (300 K) and liquid nitrogen (77 K) temperatures, with sinusoidal waveform at a frequency of 50 Hz. The stress ratio ($R$) is zero. The conventional $S$-$N$ curves of the alloy were determined. The slip patterns on the surface and fractograph were observed in JEOL T-200 and S360 scanning electron microscopes. Investigations of the microstructure by transmission electron microscopy (TEM) were performed on a PHILIPS* EM420 analytical microscope operated at 100 kV, including both thin-foil techniques and electron diffraction. The thin-foil specimen for TEM was prepared from discs cut parallel to the fracture surface, mechanically polished to a thickness of about 50 $\mu$m, and then electropolished in a solution of 30 pct nitric acid and 70 pct methanol with an electric current of 75 A at $-20$ °C.

*PHILIPS is a trademark of Philips Electronic Instruments Corporation, Mahwah, NJ.

Y.B. XU, Associate Professor, Y. ZHANG, Associate Professor, Z.G. WANG, Professor, and Q.Z. HU, Professor, are with the Laboratory of Fatigue and Fracture for Materials, Institute of Metal Research, Academia Sinica, Shenyang 110015, People's Republic of China. L. WANG is Postgraduate Student, Shenyang University of Polytechnic, Shenyang, 110021, People's Republic of China.
Manuscript submitted September 6, 1989.

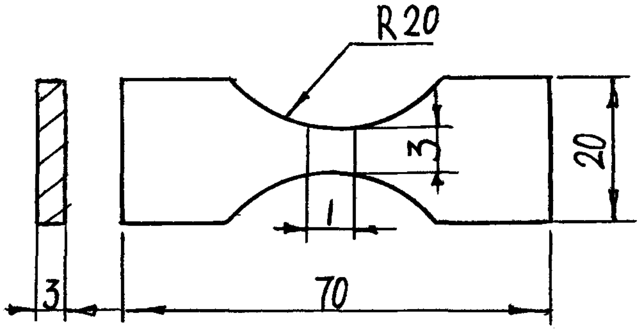


Fig. 1 — Dimensions of the fatigue specimen (in millimeters).

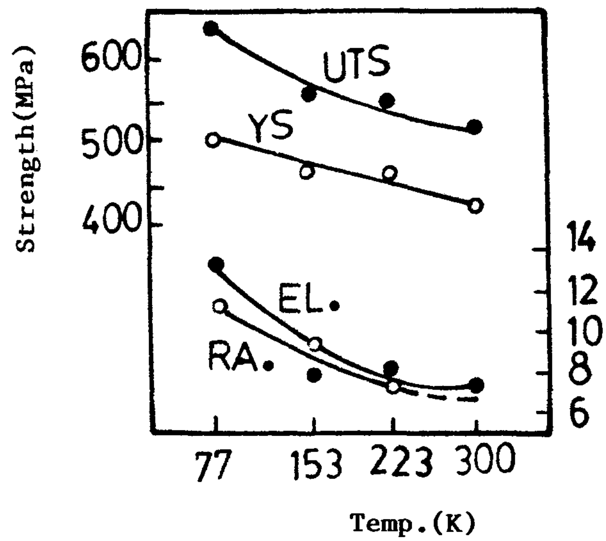


Fig. 2 — Variation of strengths and ductilities with temperature.

## III. RESULTS AND DISCUSSION

### A. *Tensile Properties*

Uniaxial tensile property data of the alloy at room and liquid nitrogen temperatures are presented in Table I and Figure 2. It can be seen clearly that yield and fracture strengths display a 10 to 20 pct increase at 77 K. It is interesting to note that the elongation value shows a larger increase of 45 pct. Thus, strength and ductility of the alloy both increase as the temperature decreases from 300 K to 77 K.

### B. *Fatigue Behavior*

The *S-N* curves for this alloy at room and liquid nitrogen temperatures are compared in Figure 3, from which some interesting results are obvious. It is found that the fatigue strength of the alloy increases markedly over the whole range of fatigue life, especially at the high-cycle fatigue range, when the temperature decreases from 300 to 77 K.

### C. *Deformation and Fracture Modes*

It is interesting to notice that the fracture at macroscopic scale occurs approximately at 45 deg to the stress axis for both uniaxial tensile and fatigue tests at room temperature (300 K). This fracture mode is similar to those found in the Cd-free Al-Li alloy in the as-quenched and underaged conditions by Lin *et al.*[7] However, at liquid nitrogen temperature (77 K), the fracture surface, in general, is roughly normal to the stress axis. Figure 4 displays a typical optical photograph of a macroetched section of fractured specimen that obtained from tensile tests. It would be expected that the effect of the temperature on the deformation mode would result from the different deformation mechanisms.

In order to confirm further the deformation mechanism, the specimen surfaces were carefully polished with diamond paste before testing. Figure 5 illustrates the conjugate shear localization formed on intersecting bands, and this alternating shear process continues, leading to a complete fracture of the specimen. It is clear that the localized deformation shear bands occur along the maximum shear stress direction.

The influence of temperature on fracture modes which affect both ductility and strength can be clearly seen from a series of fracture surface observations by scanning electron microscopy (SEM) at microscopic scale. Figure 6 shows the fractographs of typical ductile tearing (microvoid coalescence) characteristics which occur at room temperature (Figures 6(a) through (c)). However, the fracture appearance at liquid nitrogen temperature, which is different from that observed at room temperature, exhibits deeper and a larger number of delamination normal to the fracture plane, as shown in Figures 6(c) through (f).

Examinations of sections etched normal to the fracture plane by metallography reveal that this delamination occurring at low temperature has a very close relation with the cracking along intergranular or subgrain boundaries parallel to the stress axis. On the other hand, the delaminations which appeared on the fracture surface are considered to be the cracking of grain boundaries along

**Table I. Mechanical Property Data at Ambient and Low Temperatures**

| | Test Temperatures (K) | | | |
|---|---|---|---|---|
| | 77 | 153 | 223 | 300 |
| Yield strength (MPa) | 500 | 485 | 492 | 434 |
| Ultimate tensile strength (MPa) | 644 | 566 | 559 | 523 |
| Elongation (pct) | 13.0 | 7.8 | 8.0 | 7.2 |
| Reduction of area (pct) | 19.7 | 8.6 | 7.4 | — |

Note that elongation value shows a larger increase by 45 pct. Thus, strength and ductility of the alloy both increase as the temperature decreases from 300 to 77 K.

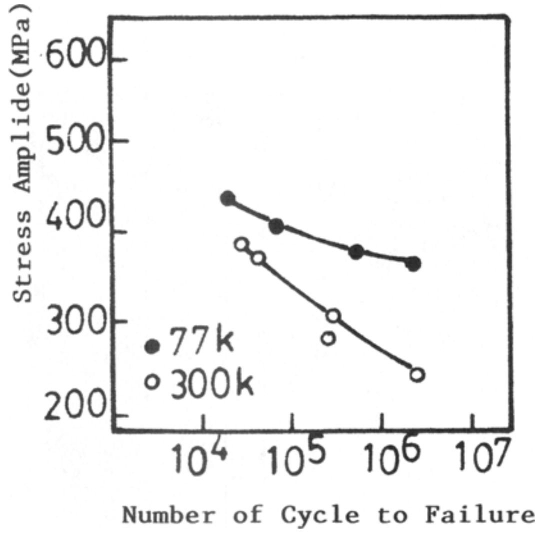


Fig. 3—*S-N* curves of the alloy fatigued at 300 and 77 K.

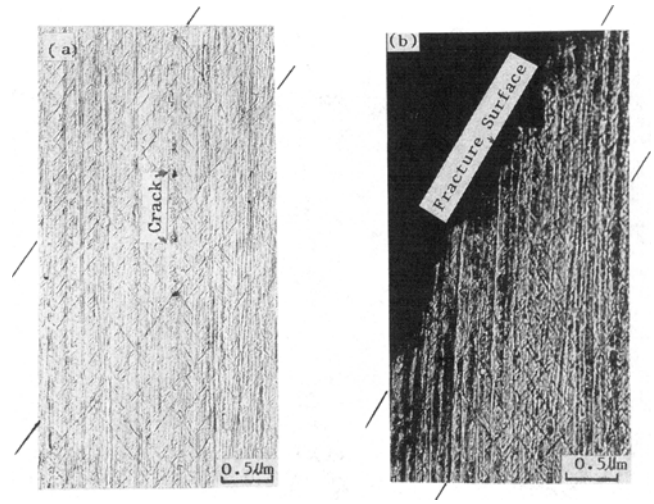


Fig. 5—(*a*) and (*b*) Localized shear deformation bands along the maximum shear stress direction occurring during the tensile test for 8090 alloy.

longitudinal direction. These observations are very similar to those obtained by Jata and Starke,[8] Venkateswara Rao and co-workers,[5,9] and Kobayashi *et al.*[10]

D. *Microstructures*

It is generally believed that the localized shear deformation leads to a failure with low toughness and low ductility during deformation at room temperature. One important aspect of the current research for aluminum-lithium alloy is the investigation on the formation and microstructures of the localized shear deformation by SEM and TEM.

Figure 7 shows a microscopic shear band occurring at room temperature. The position of the band is indicated by the arrow. It can be seen clearly that the dislocation density is extremely high compared with that out of the band, and that the tangled arrangement of dislocations tends to be aligned along the length of the shear band.

One of the interesting problems on the localized shear band is how the shear deformation develops when it crosses the grain boundary. Figure 8 indicates a localized shear crossing two different grains in orientation. The trace of the band in grain A has ⟨331⟩ direction, which coincides with the trace direction ⟨111⟩ in grain B. This suggests that the shear deformation passes through the grain boundary by multiple or cross slip systems. Figure 9 illustrates another feature of the band; *i.e.*, the traces in the bands in the adjacent grains are the same in orientation.

This implies that the localized shear deformation band propagates across the grain boundary from one grain into the adjacent grain by single slip system. Cross slip and cooperative slip are also observed frequently to form within the shear band, as shown in Figure 10. However, at liquid nitrogen temperature, the fracture mode in either

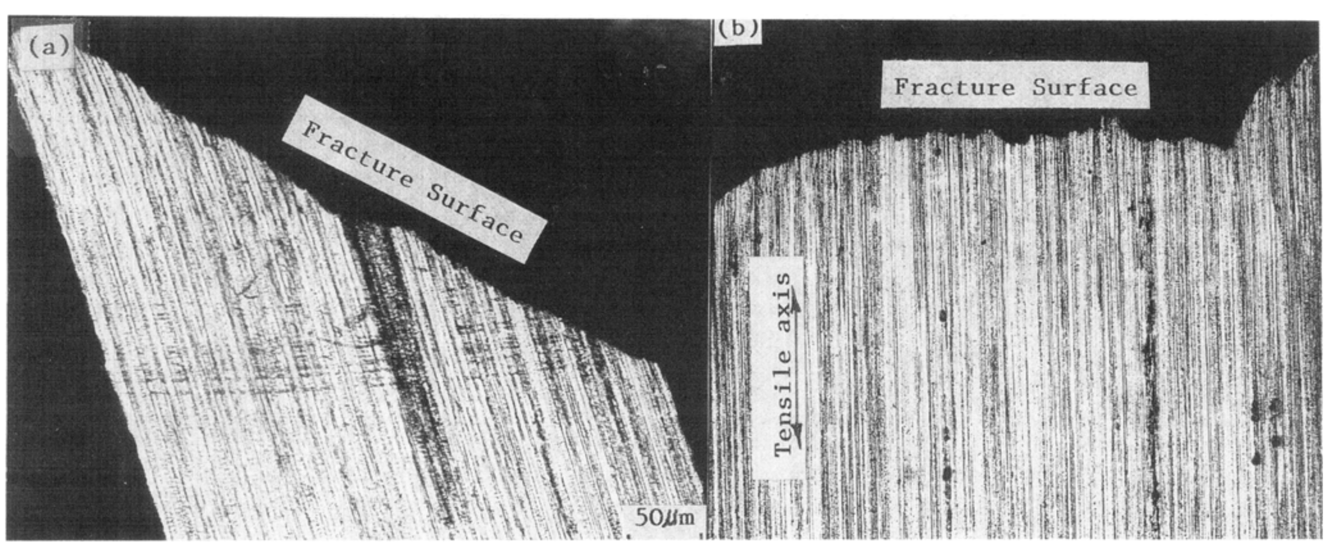


Fig. 4—Macrotopographs of fracture occurring during tensile testing at (*a*) 300 K and (*b*) 77 K.

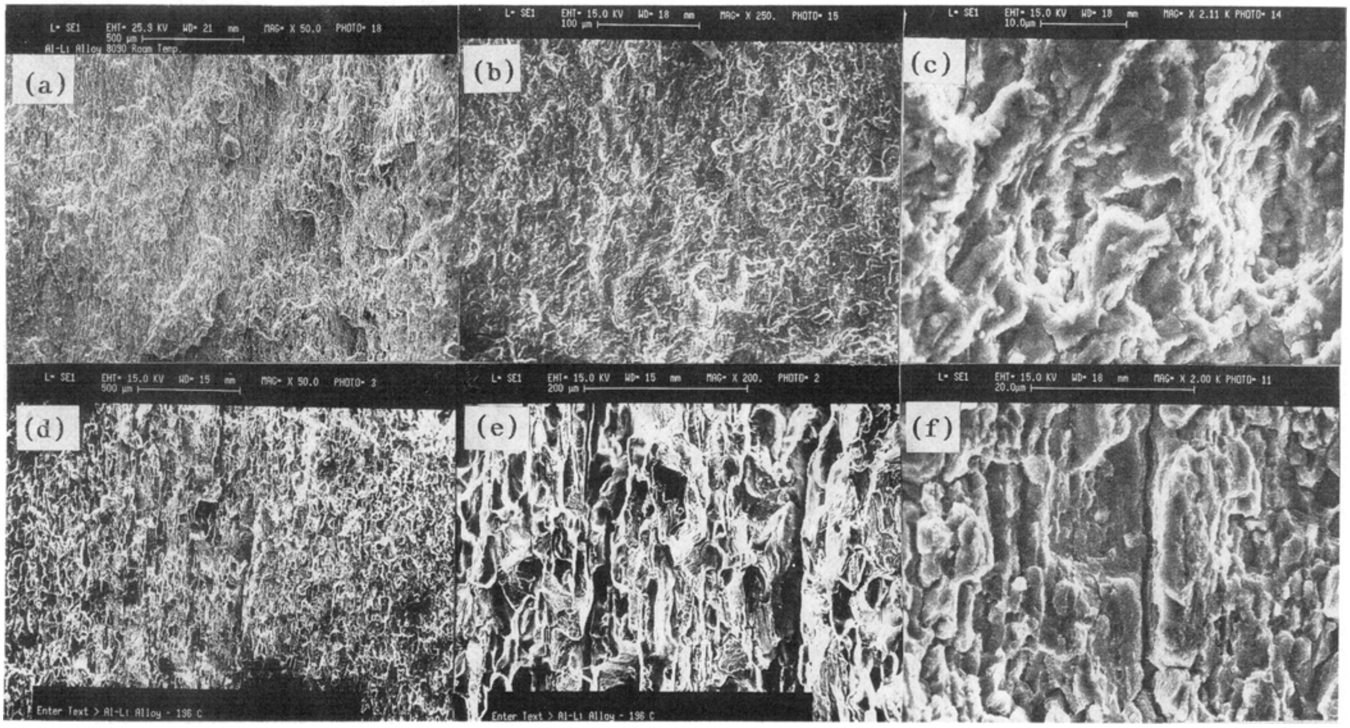

Fig. 6—Fractographs of 8090 alloy at (*a*) through (*c*) 300 K and (*d*) through (*f*) 77 K.

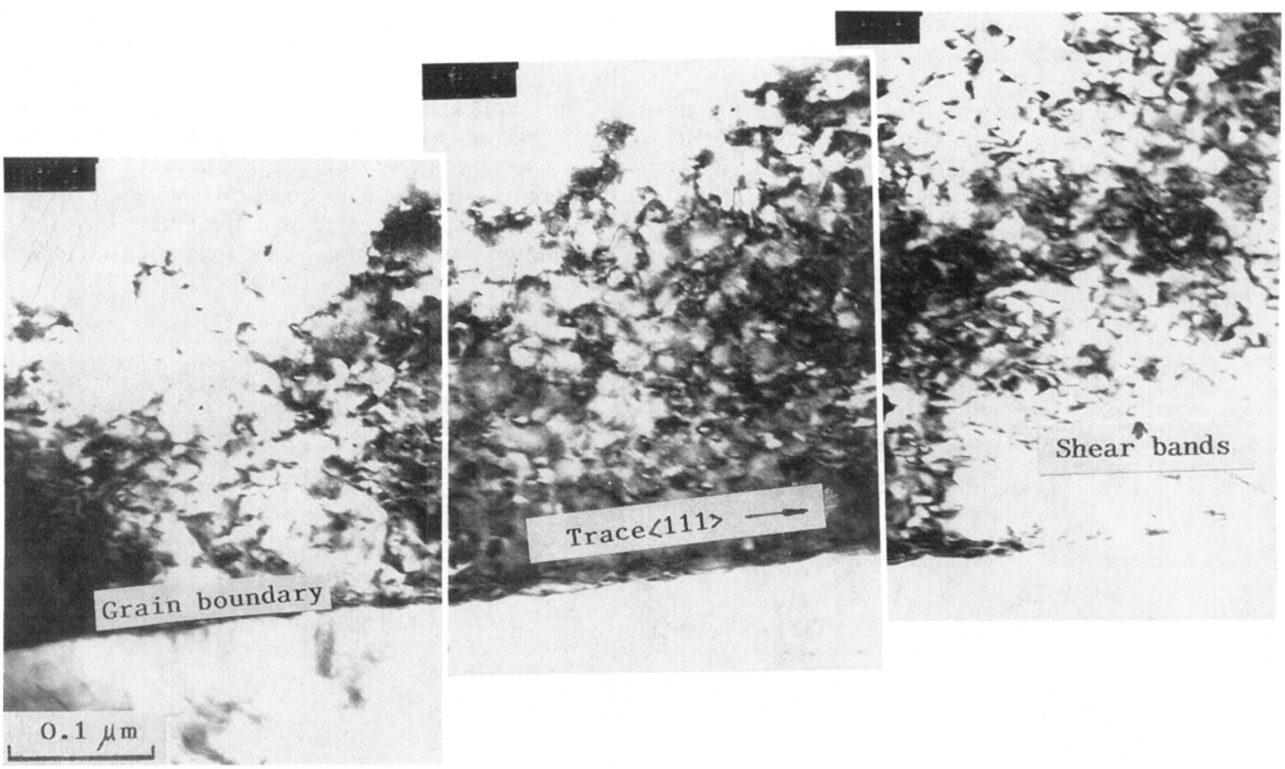

Fig. 7—TEM micrographs showing a high density of dislocations and the tangled arrangement of dislocations along the localized shear deformation band.

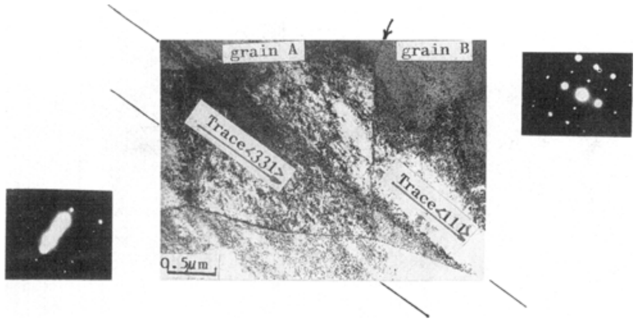


Fig. 8 — TEM micrograph from tensile specimen showing that the trace ⟨331⟩ in grain A coincides with the trace ⟨111⟩ in grain B.

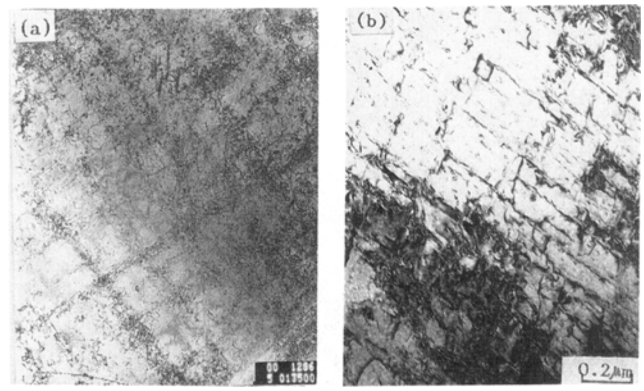


Fig. 10 — TEM micrographs showing (*a*) cross slip and (*b*) cooperative slip produced in fatigue testing corresponding to $Nf = 4.25 \times 10^5$.

fatigue or tensile test appears to be a typical ductile fracture in which the delamination feature was often observed, as mentioned earlier in this study. A detailed series of observations by TEM reveal that the dislocation density in tested specimens at liquid nitrogen temperature is much lower and distribution of dislocations is much more homogeneous in comparison with those at room temperature, as shown in Figure 11.

### E. *Interaction of $\delta'$ Precipitates with Dislocations within the Band*

It is well-known that there are two ways for dislocations to pass through the hard particles in precipitation-hardened alloys: they can either shear or bypass the hard particles.[11–16] As Sanders and Starke on Al-Li[17] and Lin *et al.* on Al-Li-Cu-Zr[7] alloys have pointed out, the low ductility for these alloys is considered attributable to intense, localized deformation. This is a result of the promotion of planar slip by coherent, shearable, hard particles and the presence of precipitate-free zones (PFZ's) at high-angle boundaries.

The present study shows that the reduction in macroscopic ductility and strength of $\delta'$-hardening aluminum-lithium alloy could be understood by the fact that moving dislocations are able to shear the ordered, coherent, and spherical $\delta'$ ($Al_3Li$) particles rather than bypass them, leading to an extreme inhomogeneous slip distribution.

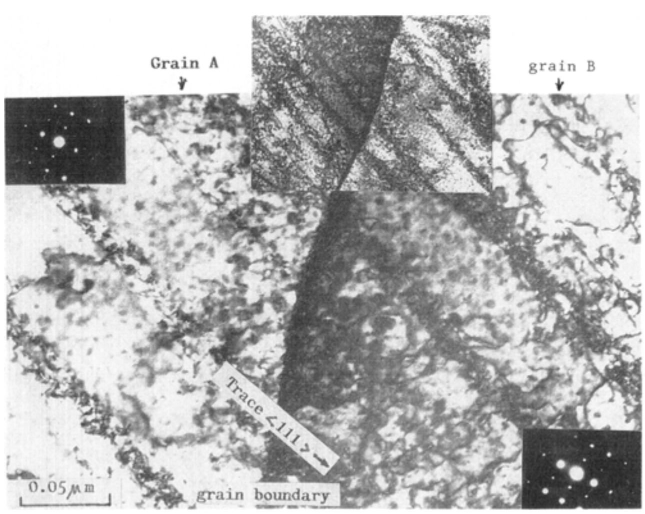


Fig. 9 — TEM micrograph indicating a localized shear crossing in the grain boundary having the same traces in orientation.

Figures 12 and 13 reveal that the hard $\delta'$ precipitates were sheared by moving dislocations along the length of the band into two or three parts, which is similar to that found by Khireddine *et al.*[18] on low-cycle fatigue properties of an aluminum-lithium alloy (Al-Li-Cu-Mg-Zr).

It is obvious that the stress concentration arising from the high localized shear deformation can easily initiate a microcrack within the band. This situation can be seen clearly in Figure 14, where a microcrack propagates along the shear band at room temperature.

From experimental results mentioned above, it would be expected that the observed reduction in fatigue and fracture strengths as well as ductilities at room temperature compared with those at liquid nitrogen temperature for Al-Li-Cu-Mg-Zr 8090-T6 alloy can be explained in terms of the increase in tendency for homogeneous slip. The localization of plastic deformation into a very narrow slip band leads to high stress concentration and, in turn, favors microstructure damage, as evidenced by crack nucleation and growth as well as hard $\delta'$ precipitates cut by moving dislocations in the band. In other words, the reduction in fatigue and fracture strengths, as well as ductilities at room temperature is attributed to the occurrence of the localized shear deformation band in which the hard $\delta'$ precipitates are sheared by moving dislocations. However, the improvement in fatigue and fracture strengths as well as ductilities of the alloy at liquid nitrogen temperature, is considered to be the result of "delamination toughening" which was proposed by Venkateswara Rao *et al.*,[19] who pointed out that such delamination can increase the degree of in-plane crack deflection, which provides a further contribution to toughening of the alloy.[9]

It should be pointed out that the formation and development of the localized shear, leading to the reduction in ductility and toughness of the Al-Li alloy, are very complex deformation processes which involve a variety of phenomena, such as the changes in orientation, hardening, and softening, as well as destruction of coherent, ordered $\delta'$ particles within the band. Sometimes, these events occurring in the band are almost catastrophic. Since it is rather difficult to follow the formation

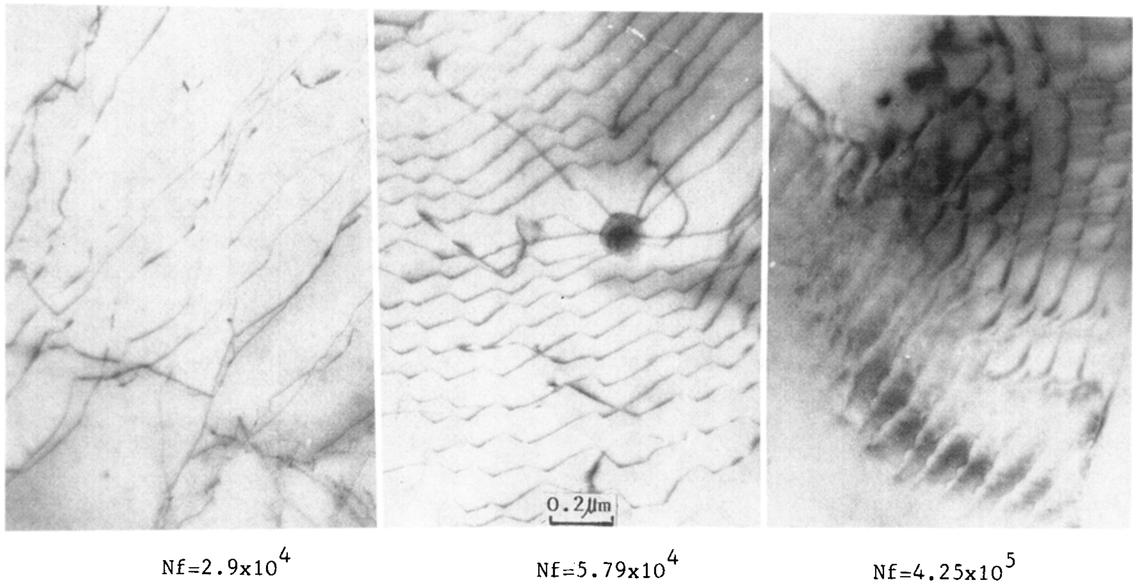


Fig. 11—TEM micrographs from fatigue tests at 77 K showing dislocation substructures.

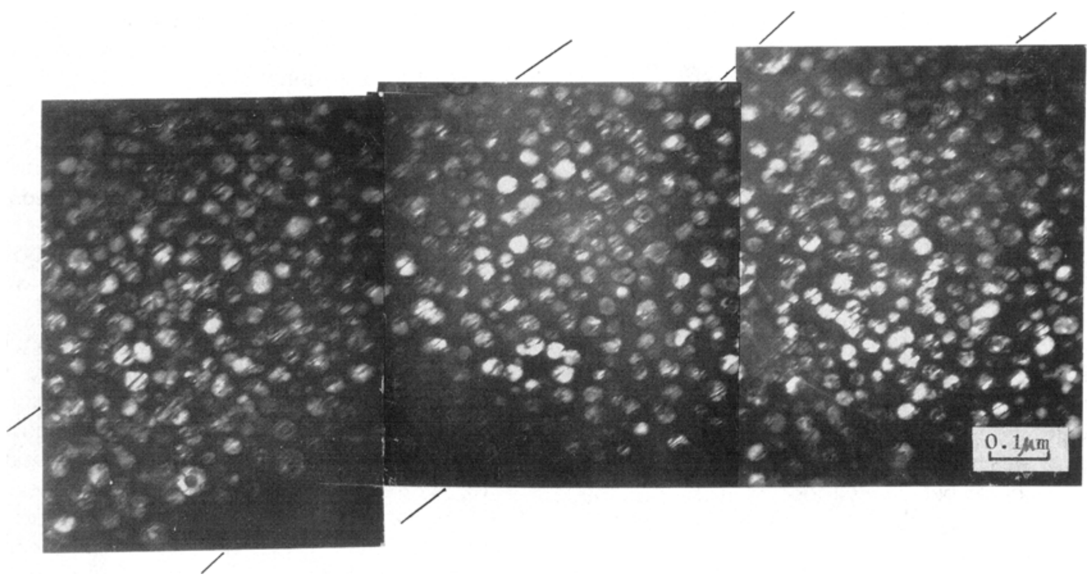


Fig. 12—δ′ phases were sheared by moving dislocations within the localized shear band occurring during fatigue tests at 300 K for 8090 alloy (dark field).

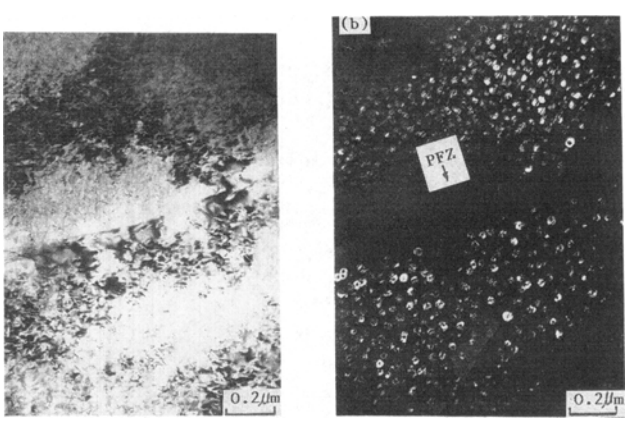


Fig. 13—δ′ particles and PFZ in the shear deformation band: (*a*) bright field and (*b*) dark field.

and development of each event during deformation, further work on basic phenomena at both macro- and microscopic scales is still needed.

## IV. CONCLUSIONS

Based on a study of the fatigue and fracture behavior of Al-Li-Mg-Cu-Zr alloy 8090-T6 at both ambient and cryogenic temperatures, the following conclusions can be drawn:

1. The fatigue strength of Al-Li-Mg-Cu-Zr alloy 8090-T6 increases as the test temperature decreases, especially in the long life regime.
2. Changes in fatigue and fracture strengths are considered to be associated with the deformation modes.

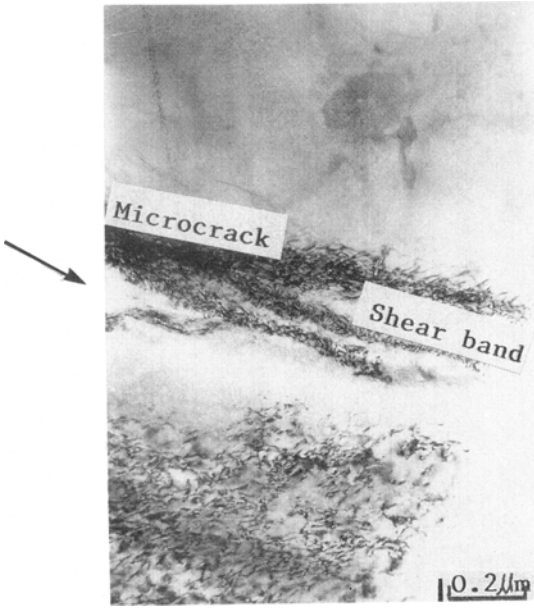


Fig. 14—TEM micrograph showing a fatigue crack propagating along the localized shear band at 300 K ($Nf = 1.48 \times 10^6$).

The fracture at liquid nitrogen temperature exhibits deeper and larger numbers of delaminations which seem to disperse the strain concentration, leading to the shear deformation localization. However, at room temperature, fracture, in either fatigue or uniaxial tensile tests, appears to be the cracking along the localized shear bands.

3. The impairment of the fatigue and fracture strengths as well as ductilities of Al-Li-Mg-Cu-Zr alloy 8090-T6 at room temperature compared with those at liquid nitrogen temperature might be attributed to the occurrence of the localized shear deformation band in which the hard $\delta'$ precipitates are sheared by moving dislocations.

## ACKNOWLEDGMENT

This work was supported by the Chinese Academy of Sciences. The authors are very grateful for this support.

## REFERENCES

1. D.C. Dorward: *Scripta Metall.*, 1986, vol. 20, pp. 1379-83.
2. J. Glazer, S.L. Verzasconi, R.R. Sawtell, and J.W. Morris, Jr.: *Metall. Trans. A*, 1987, vol. 18A, pp. 1695-1701.
3. D. Webster: *Metall. Trans. A*, 1987, vol. 18A, pp. 2181-93.
4. K.V. Jata and E.A. Starke, Jr.: *Metall. Trans. A*, 1986, vol. 17A, pp. 1011-26.
5. K.T. Venkateswara Rao, H.F. Hayashigatani, W. Yu, and R.O. Ritchie: *Scripta Metall.*, 1988, vol. 22, pp. 93-98.
6. Y.B. Xu, Z.G. Wang, Y. Zhang, H.H. Zhao, and Z.Q. Hu: *Proc. 5th Int. Al-Li Conf.*, Williamsburg, Virginia, Mar. 27–31, 1989, T.H. Sanders, Jr. and E.A. Starke, Jr., eds., Materials and Component Engineering Publications Ltd., Birmingham, U.K., vol. II, pp. 1147-1151.
7. F.S. Lin, S.B. Chakrabortty, and E.A. Starke, Jr.: *Metall. Trans. A*, 1982, vol. 13A, pp. 1401-10.
8. K.V. Jata and E.A. Starke, Jr.: *Scripta Metall.*, 1988, vol. 22, pp. 1553-56.
9. K.V. Venkateswara Rao, H.F. Hayashigatani, W. Yu, and R.O. Ritchie: *Scripta Metall.*, 1988, vol. 22, pp. 93-98.
10. T. Kobayashi, M. Niinomi, and K. Dsgawa: *Mater. Sci. Technol.*, 1989, vol. 5, pp. 1013-19.
11. J. Lendvai, H.J. Gudladt, and V. Gerold: *Scripta Metall.*, 1988, vol. 22, pp. 1755-60.
12. J. Th. M. De Hosson, A. Huisint Veld, H. Tamler, and O. Kanert: *Acta Metall.*, 1984, vol. 32, pp. 1205-15.
13. A.K. Vasudevan and R.D. Doherty: *Acta Metall.*, 1984, vol. 32, pp. 1193-1219.
14. S. Horibe and C. Laird: *Acta Metall.*, 1987, vol. 35, pp. 1919-27.
15. R.E. Crooks, E.A. Kenik, and E.A. Starke, Jr.: *Scripta Metall.*, 1983, vol. 17, pp. 643-47.
16. J. Glazer and J.W. Morris, Jr.: *Phil. Mag.*, 1987, vol. 56, p. 507.
17. T.H. Sanders, Jr. and E.A. Starke, Jr.: *Acta Metall.*, 1982, vol. 30, pp. 927-39.
18. D. Khireddine, R. Rahouadj, and M. Clavel: *Acta Metall.*, 1989, vol. 37, pp. 191-201.
19. K.T. Venkateswara Rao, H.F. Hayashigatani, W. Yu, and R.O. Ritchie: *Scripta Metall.*, 1988, vol. 22, pp. 93-98.